Electron-Induced Cascade Showers in Water and Aluminum*

CAROL JO CRANNELL AND HALL CRANNELL
Department of Physics, The Catholic University of America, Washington, D. C. 20017
AND
RANDY R. WHITNEY AND H. D. ZEMAN
High Energy Physics Laboratory, Stanford University, Stanford, California 94305
(Received 30 January 1969)

In the present experiment, the three-dimensional distribution of energy deposition was measured for 1-GeV electron-induced showers in water and aluminum. For the water target, two different detectors were employed: CsI(Tl) and anthracene. The measured longitudinal distribution of energy in water was found to be essentially independent of the detector employed in the measurement, while the radial distribution of energy deposition shows a strong detector dependence. Data were measured for the aluminum target with a CaF_2(Eu) detector. All of these data support the description that the primary energy-deposition mechanism at the initiation of the shower is ionization of the target material, and that the principle energy-transport mechanism after shower maximum is the propagation of minimum-attenuation γ rays. The radial distributions of energy deposition show that the apparent dependence on the atomic number of the target observed in an earlier experiment was in part a detector-dependent result. The radial distributions nevertheless show significant differences from the prediction based on the Monte Carlo calculations of Nagel.

INTRODUCTION

THE lateral and longitudinal distributions of energy deposition in electromagnetic cascade showers are of particular practical interest for media typically used as radiation shielding materials. In the present experiment, showers were initiated by electrons with 1-GeV incident energy. Recently, improved experimental techniques have been employed to measure the lateral and longitudinal distribution of energy deposition in targets of low atomic number. Data have been measured for a water target with both anthracene and CsI(Tl) detectors and for an aluminum target with a CaF_2(Eu) detector. The anthracene and CaF_2(Eu) detectors were chosen to match as nearly as possible the effective atomic numbers of the respective target media. The CsI(Tl) detector was employed to obtain data for a comparison with previous results which indicated an apparent dependence of the radial distribution of energy deposition on the atomic number of the target.

The principle processes responsible for the cascade shower phenomena have been discussed by Rossi.[1] An analytic treatment of the longitudinal behavior of showers has been developed by Rossi and Greisen.[2] Many other calculations, both analytic and Monte Carlo,[3] have been performed on various characteristics of both the lateral and the longitudinal aspect of cascade showers. Recently, a Monte Carlo program was developed by Nagel[4] to calculate both the longitudinal and the radial properties of showers, in which lower energy partitioning of the shower is considered than in previous work. The results obtained in this experiment are compared with the results obtained by Nagel.

Kantz and Hofstadter,[5,6] using scintillation detectors, obtained the first measurements of the radial, as well as the longitudinal, deposition of energy in an electron-induced shower. Carbon, aluminum, copper, tin, and lead were investigated using electrons with incident energy of 185 MeV. The technique employed in this experiment is similar to that developed by Kantz and Hofstadter.

The improved experimental apparatus and data-acquisition procedure employed in this work have been described previously[7,8] and are briefly discussed in the next section. The results are presented in tabular and graphic form, and the interpretation of these results in light of previous data and theoretical predictions is discussed.

EXPERIMENTAL TECHNIQUE

In Table I, the numerical parameters associated with the target materials are presented. The water target

* Work supported in part by the U. S. Office of Naval Research Contract No. Nonr 225(67) and Contract No. N00014-67-A-0377-0002.

[1] B. Rossi, *High-Energy Particles* (Prentice-Hall, Inc., Englewood Cliffs, N. J., 1952).

[2] B. Rossi and K. Greisen, Rev. Mod. Phys. **13**, 240 (1941).

[3] For references to many of the analytical calculations performed before 1959, see K. Kamata and J. Nishimura, Progr. Theoret. Phys. Suppl. **6**, 93 (1958); S. Z. Blen'kii and I. P. Ivanenko, Usp. Fiz. Nauk **69**, 591 (1959) [English transl.: Soviet Phys.—Usp. **2**, 912 (1960)]. Also see O. I. Dovzhenko and A. A. Pomanskii, Zh. Eksperim. i Teor. Fiz. **45**, 268 (1963) [English transl.: Soviet Phys.—JETP **18**, 187 (1964)]. For references to the prominent Monte Carlo calculations, see C. Crannell, Phys. Rev. **161**, 310 (1967).

[4] H. Nagel, Z. Physik **186**, 319 (1965); for calculations applying Nagel's program to showers initated by higher-energy incident particles, see U. Volkel, Report No. DESY 65/6, 1965 (unpublished); Report No. DESY 67/16, 1967 (unpublished).

[5] A. Kantz, Ph.D. thesis, Stanford University, 1954 (unpublished); Stanford University, High Energy Physics Laboratory Report No. 17, 1954 (unpublished).

[6] A. Kantz and R. Hofstadter, Phys. Rev. **89**, 607 (1953); Nucleonics **12**, 36 (1954).

[7] C. Crannell, Ph.D. thesis, Stanford University, 1967 (unpublished); Phys. Rev. **161**, 310 (1967).

[8] M. R. Yearian, C. J. Crannell, H. Crannell, D. C. Smith, P. J. Friedl, C. Sederholm, and W. Dye, IEEE Trans. Nucl. Sci. **NS-14**, 608 (1967).

consisted of a steel tank containing 8000 liters of distilled water. The movable detector assembly was mounted on tracks above the tank. The incident beam entered the water through a 0.13-mm-thick aluminum window which was centered on the square end of the tank. The entire detector assembly could be moved by remote control both along the direction of the incident beam and perpendicular (horizontally) to the direction of the incident beam. The probe itself could be moved remotely in a direction perpendicular (vertically) to the incident beam. The probe consisted of a photomultiplier tube optically coupled to a detector of anthracene or CsI(Tl) by means of a Lucite and polished aluminum light guide. Details of the construction of the target and detector assemblies[7] and the closed-loop data-acquisition technique[8] have been described previously.

A pulsed beam of 1-GeV electrons was normally incident on the target at a repetition rate of 60 Hz. The energy of the incident electrons was known to 0.5% and the momentum spread in the beam was 0.2%. The signal from the probe was amplified, converted to a digital signal, and automatically read by an on-line data-acquisition system after each burst of electrons from the accelerator. A gas Čerenkov monitor[9] was employed to measure the intensity of each accelerator burst. The signal from the monitor was similarly amplified, digitized, and read by the computer. At each probe position, the signals were measured and the ratio of probe to monitor signal was calculated until a sufficient number of measurements were made to ensure that a statistical accuracy commensurate with the other experimental parameters was obtained. The data acquisition system then printed out the numerical value of the ratio of the probe signal to monitor signal, plotted the ratio as a function of the radial distance of the probe from the beam axis, and moved the probe to a new radial position which was determined from the rate of change of the ratio and the size of the previous radial increment.

The aluminum target was composed of plates varying in thickness from 0.64 to 2.5 cm. The plates were pressed together to simulate a solid target of the dimensions given in Table I. The probe could be moved remotely only in a direction perpendicular to the incident beam. The detector employed with the aluminum target was a CaF_2(Eu) pellet. The atomic numbers associated with the detectors used in this experiment are listed in Table II.

The data-reduction techniques also have been described previously.[7] The measured energy deposition as a function of the lateral and longitudinal position of the probe was reduced and analyzed with the assistance of an IBM 7090 computer. The three-dimensional distribution of energy deposition for water as determined with anthracene and CsI(Tl) detectors and for aluminum with a CaF_2(Eu) detector was obtained by a numerical integration of the radial distribution curves.

[9] C. Crannell, H. Crannell, and H. Zeman, Rev. Sci. Instr. **40**, 661 (1969).

TABLE I. Numerical parameters associated with the target materials.

Target material	Atomic number	Dimensions of target (cm^3)	Density ($g\ cm^{-3}$)	Radiation length[a] ($g\ cm^{-2}$)	Critical energy[a] (MeV)
Aluminum	13	61×61×180	2.7	24.3	40.0
Water	1, 8	122×122×460	1.0	36.4	73.0

[a] Calculated using Eq. 5.2(1) of Rossi (Ref. 1), and found to be in good agreement with the corresponding values given by O. I. Dovzhenko and A. A. Ponamskii, Zh. Eksperim. i Teor. Fiz. **45**, 268 (1963) [English transl.: Soviet Phys.—JETP **18**, 187 (1964)].

RESULTS

The fraction of the incident energy deposited as a function of depth is determined from an integration of the measured radial distribution of energy. A plot of the energy deposited per unit depth as a function of the depth is called a transition curve. The transition curves measured for water with anthracene and CsI(Tl) detectors are shown in Fig. 1(a). The transition curve measured for aluminum with a CaF_2(Eu) detector is shown in Fig. 1(b). Each of the three sets of measurements has been normalized so that the total area under each transition curve is equal to unity. The uncertainties in the data presented in Figs. 1(a) and 1(b), due to the inherent limitations of the experimental equipment, are ±3% in the energy deposition, ±0.5 cm in the depth for water, and −0.08 +0.32 cm in the depth for aluminum. Systematic effects depending on the symmetry of the incident beam and the size of the detector are expected to affect the determination of the transition curve at the zero depth point by no more than ±25% in water and ±30% in aluminum. Near shower maximum and beyond, these effects are expected to be negligible. At depths beyond shower maximum the integration of the radial distribution of energy employed an extrapolation of the data beyond the greatest measured radius. The fraction of the integral which depended on the extrapolation was never more than 30%, and is believed to contribute to an uncertainty in the transition curve at great depths of no more than ±10%.

TABLE II. Atomic numbers of the principle constituents[a] of the detectors used in this experiment.

Detector	Atomic numbers
Anthracene $C_6H_4:(CH)_2:C_6H_4$	6, 1
CaF_2(Eu)	20, 9
CsI(Tl)	55, 53

[a] The europium (Eu) and the thallium (Tl) are present only in trace amounts and should not significantly affect the energy stopping properties of the detectors.

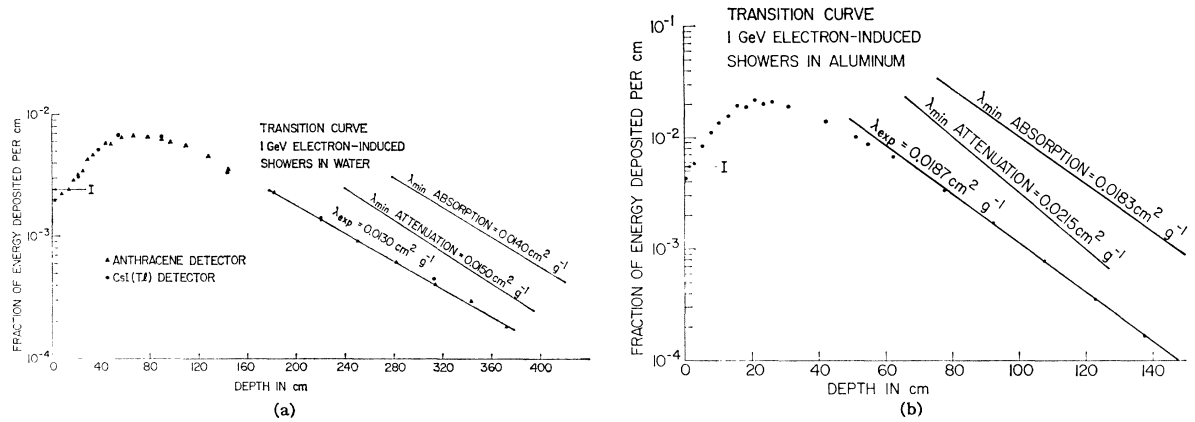

FIG. 1. Experimentally determined transition curves for 1-GeV electron-induced showers in water and aluminum. The fraction of the incident energy deposited per unit depth is plotted as a function of the depth in centimeters. The arrow labeled "I" indicates the value calculated by Sternheimer for the energy lost per cm through ionization of the target material by 1-GeV electrons. The quantity λ_{expt} for each transition curve is determined by a least-squares fit of the data. The lines drawn with λ_{min} absorption and λ_{min} attenuation illustrate the slopes associated with these coefficients.

The arrows labeled "I" in Figs. 1(a) and 1(b) indicate the energy deposition per unit depth that would be expected from ionization of the target media by 1-GeV electrons. Since ionization of the target medium is the dominant mechanism by which energy is deposited at the initiation of the shower, it is expected that the transition curve should assume this value at zero depth. Agreement with the ionization loss rate calculated by Sternheimer[10] is obtained to within the systematic uncertainties associated with the measurements. The results are also presented in Table III.

Since the most penetrating component of a shower is minimum-attenuation γ rays, it was suggested earlier,[11] and verified by subsequent experiments,[5–7,12–14] that one might expect the transition curve to decrease exponentially at a rate approximately determined by the minimum-attenuation coefficient for γ rays in the particular target material. The experimentally determined rates of decrease as well as the slopes associated with the minimum attenuation and absorption coefficients are shown graphically in Figs. 1(a) and 1(b). The measured rates were determined by a least-squares fit of the data taken well past shower maximum and are given in Table IV along with the related experimental uncertainties.

The data were further analyzed to determine the lateral distribution of energy deposition, integrated over all depths. These results were then used to calculate the fraction of the energy that would escape a cylinder of semi-infinite length as a function of the radius of the cylinder. The results for this experiment are shown as "radial escape curves" in Fig. 2. For comparison, the results for a 900-MeV electron-induced shower in tin from a previous experiment[7] and for a 950-MeV electron-induced shower in lead from the Monte Carlo calculations of Nagel[4] are shown.

The experimentally determined lateral and longitudinal distributions of energy deposition for 1-GeV electron-induced showers in water measured with the anthracene detector and in aluminum measured with the CaF_2(Eu) detector are presented in Tables V–VIII. The differential energy block diagrams display the percentage of the incident energy deposited in a cylindrical ring between the indicated radii and depths. The integral energy block diagrams display the percentage of the incident energy deposited in an entire cylindrical section of the indicated radius and depth.

DISCUSSION

Longitudinal Development

The results of this experiment for the longitudinal distribution of energy deposition show the same general behavior as found in previous experiments.[5–7,12–14] However, the results of all of the experiments considered together show an atomic-number-dependent characteristic.

TABLE III. Energy lost by ionization in MeV cm^2 g^{-1}.

Target Material	Sternheimer[a] Calculated for 1-GeV incident electrons	This experiment 1-GeV incident electrons
Aluminum	2.02	1.5 ±0.5
Water	2.40	1.95±0.5

[a] R. M. Sternheimer, Phys. Rev. 88, 851 (1952); 91, 256 (1953); 103, 511 (1956).

[10] R. M. Sternheimer, Phys. Rev. **88**, 851 (1952); **91**, 256 (1953); **103**, 511 (1956).
[11] K. Greisen, Phys. Rev. **75**, 1071 (1949).
[12] W. Blocker, R. Kenney, and W. Panofsky, Phys. Rev. **79**, 419 (1950).
[13] H. Thom, Phys. Rev. **136**, B447 (1964).
[14] W. Nelson, T. Jenkins, R. McCall, and J. Cobb, Phys. Rev. **149**, 201 (1966).

It was suggested by Kantz and Hofstadter[5,6] that at the start of an electromagnetic cascade the energy deposited per unit depth in the target material should correspond to that fraction of the incident energy lost per unit depth by the incident electrons through ionization of the target media. To within the experimental uncertainties, the measured rate of energy deposition at zero depth corresponds to the energy lost by 1-GeV electrons through ionization of the respective target materials as calculated by Sternheimer.[10]

In previous experiments,[7] the transition curves were found to decrease at a rate which was less than the rate at which minimum attenuation γ rays are attenuated and greater than the rate at which energy is absorbed from a beam of minimum absorption γ rays. When the data measured previously with 900-MeV electron-induced showers in copper, tin and lead are considered together with the results of the present experiment for 1-GeV electron-induced showers in water and aluminim, an atomic-number–dependent effect is observed. The agreement is better with the attenuation coefficient, the higher the atomic number of the target material, and with the absorption coefficient, the lower the atomic number of the material. These observations are consistent with a model suggested previously.[7] In materials of high atomic number, in which the minimum in the attenuation curve is relatively sharp, the γ ray rapidly gives up all its energy to the media as soon as it suffers any collision. In materials of lower atomic number, in which the minimum occurs at higher energy and is relatively broadened, the attenuated γ ray may still propagate its energy to significantly greater depths. The rate of energy deposition then more closely approximates the rate of energy absorption at the minimum in the absorption curve. The knowledge of this behavior over a wide range of atomic numbers provides us with a more complete picture of the energy transport and deposition mechanisms at depths beyond shower maximum.

In the present experiment, the transition curve in water was measured independently with two different detectors. One detector, anthracene, has an effective atomic number approximately the same as that of water. The other detector CsI(Tl) has an effective atomic number which is much greater (see Table II). The stopping power of anthracene for all the shower particles, from high-energy electrons to low-energy γ rays, is expected to be similar to that of water. The relative stopping power of CsI(Tl) for low-energy γ rays, however, is expected to be much greater than the stopping power for high-energy electrons. It is surprising, therefore, that the energy deposition measured with the CsI(Tl) detector is not significantly greater in the tail of the transition curve and less in the region before shower maximum.

TABLE IV. Comparison of experimentally determined coefficients with γ-ray absorption and attenuation coefficients.

Target element	λ_{min}[a] Absorption $cm^2\ g^{-1}$	λ_{min}[a] Attenuation $cm^2\ g^{-1}$	λ_{expt} $cm^2\ g^{-1}$
Aluminum	0.0183	0.0215	0.0187±0.0006
Water	0.0140	0.0150	0.0130±0.0005

[a] W. S. Snyder and J. L. Powell, Oak Ridge National Laboratory Report No. ORNL 421, 1950 (unpublished); also quoted in O. I. Leipunskii, B. V. Novozhilov, V. N. Sakharov, *The Propagation of Gamma Quanta in Matter*, translated by Prasenjit Basu, 1st English edition edited by K. T. Spinney, J. Butler, and J. B. Sykes, (Pergammon Press, Oxford, 1965).

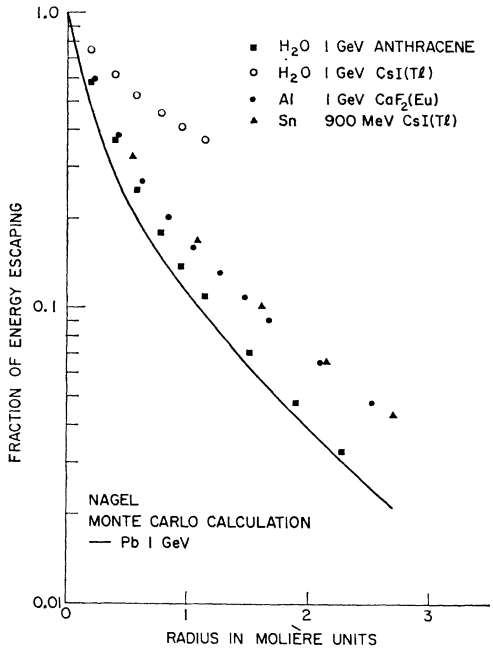

FIG. 2. Radial escape curves. The fraction of the incident energy escaping from an infinitely long cylinder is plotted as a function of the radius in Molière units. The data from the present and the previous experiments are compared with the Monte Carlo calculations by Nagel for 1-GeV electron-induced showers in lead. The values for the radiation length and the critical energy, used in calculating the Molière length for water and aluminum, are given in Table I.

Lateral Development

Radial escape curves, calculated from the lateral distribution of energy deposition, are presented in Fig. 2. For the water target, the data measured with a CsI(Tl) detector indicate a much greater radial spread of energy than do the data measured with the anthracene detector. To the extent that the effective atomic number of anthracene is the same as the effective atomic number of water, it is expected that the lateral distribution of energy deposition measured with the anthracene detector presents an accurate picture of the energy actually deposited in the water target itself. The effective atomic number of CsI(Tl) is much larger than that of water (see Tables I and II). It is not surprising that the data measured with the CsI(Tl) detector show significant differences from those measured with anthracene.

TABLE V. Differential energy block diagram 1-GeV electron-induced showers in water.

Radius in cm	Depth in cm 0–20	20–40	40–60	60–80	80–120	120–160	160–200	200–240	240–280	280–320	320–360	360–∞
24–∞	0.06	0.07	0.09	0.11	0.32	0.46	0.50	0.44	0.38	0.30	0.23	0.31
20–24		0.02	0.03	0.05	0.17	0.25	0.25	0.22	0.17	0.12	0.08	0.18
16–20	0.01	0.02	0.04	0.08	0.28	0.41	0.40	0.33	0.24	0.17	0.11	0.20
12–16		0.03	0.07	0.14	0.55	0.78	0.70	0.54	0.37	0.24	0.15	0.23
8–12	0.01	0.06	0.18	0.37	1.41	1.67	1.33	0.92	0.58	0.35	0.20	0.26
6–8	0.01	0.07	0.24	0.51	1.70	1.65	1.14	0.69	0.40	0.22	0.12	0.14
4–6	0.02	0.20	0.63	1.21	3.38	2.66	1.61	0.88	0.47	0.25	0.13	0.13
3–4	0.03	0.24	0.69	1.23	2.86	1.83	0.98	0.49	0.25	0.12	0.06	0.06
2–3	0.07	0.50	1.34	2.17	4.03	2.18	1.03	0.48	0.23	0.11	0.05	0.05
1–2	0.22	1.28	3.14	3.86	5.03	2.16	0.92	0.40	0.18	0.08	0.04	0.03
0–1	4.41	6.13	5.57	3.53	3.32	1.16	0.45	0.18	0.08	0.04	0.02	0.01

TABLE VI. Integral energy block diagram 1-GeV electron-induced showers in water.

Radius in cm	Depth in cm 0–20	20–40	40–60	60–80	80–120	120–160	160–200	200–240	240–280	280–320	320–360	360–∞
24–∞	4.85	13.5	25.5	38.7	61.8	77.0	86.3	91.9	95.2	97.2	98.4	100.0
20–24			25.3	38.4	61.1	75.9	84.7	89.8	92.8	94.5	95.4	96.7
16–20	4.78	13.3	25.2	38.3	60.9	75.4	83.9	88.8	91.6	93.2	94.1	95.2
12–16				38.2	60.4	74.5	82.7	87.3	89.8	91.2	92.0	92.9
8–12	4.77	13.2	25.0	37.9	59.6	73.0	80.4	84.4	86.6	87.8	88.4	89.1
6–8	4.76	13.2	24.8	37.3	57.6	69.2	75.4	78.5	80.1	80.9	81.3	81.8
4–6	4.75	13.1	24.5	36.5	55.1	65.1	70.0	72.5	73.7	74.3	74.6	74.9
3–4	4.73	12.9	23.6	34.4	49.6	57.0	60.3	61.9	62.6	63.0	63.2	63.3
2–3	4.70	12.6	22.7	32.2	44.6	50.1	52.5	53.6	54.1	54.3	54.4	54.5
1–2	4.62	12.0	20.7	28.1	36.5	39.8	41.2	41.8	42.0	←42.2→		42.3
0–1	4.41	10.5	16.1	19.6	23.0	24.1	24.6	←24.8→		←24.9→		

TABLE VII. Differential energy block diagram 1-GeV electron-induced showers in aluminum.

Radius in cm	Depth in cm 0–10	10–20	20–30	30–40	40–50	50–60	60–70	70–80	80–90	90–100	100–120	120–∞
12–∞	0.05	0.17	0.32	0.51	0.64	0.67	0.59	0.53	0.41	0.32	0.42	0.43
10–12	0.02	0.07	0.14	0.21	0.26	0.26	0.22	0.18	0.13	0.09	0.10	0.06
8–10	0.03	0.10	0.22	0.32	0.39	0.39	0.31	0.26	0.18	0.13	0.14	0.07
7–8	0.02	0.07	0.16	0.24	0.28	0.27	0.22	0.17	0.12	0.08	0.08	0.04
6–7	0.02	0.09	0.21	0.33	0.37	0.36	0.27	0.21	0.14	0.10	0.09	0.04
5–6	0.03	0.13	0.31	0.48	0.53	0.45	0.35	0.26	0.17	0.11	0.10	0.05
4–5	0.04	0.20	0.52	0.76	0.79	0.63	0.47	0.34	0.21	0.13	0.12	0.05
3–4	0.06	0.40	0.98	1.33	1.26	0.93	0.65	0.44	0.26	0.15	0.13	0.05
2–3	0.13	0.96	2.14	2.51	1.91	1.37	0.88	0.55	0.30	0.17	0.14	0.05
1–2	0.45	2.94	5.29	4.86	3.07	1.88	1.07	0.60	0.32	0.17	0.13	0.04
0–1	7.42	12.2	10.1	5.57	2.89	1.45	0.72	0.36	0.17	0.08	0.06	0.02

TABLE VIII. Integral energy block diagram 1-GeV electron-induced showers in aluminum.

Radius in cm	Depth in cm 0–10	10–20	20–30	30–40	40–50	50–60	60–70	70–80	80–90	90–100	100–120	120–∞
12–∞	8.25	25.6	46.0	62.8	75.3	84.1	89.9	93.8	6.2	97.7	99.2	100.0
10–12	8.21	25.4	45.5	62.1	73.9	81.9	87.0	90.4	92.4	93.6	94.7	95.2
8–10	8.19	25.3	45.3	61.7	73.2	80.9	85.8	89.0	90.9	92.0	93.0	93.4
7–8	8.16	25.2	44.9	61.0	72.1	79.5	84.1	87.0	88.7	89.7	90.6	90.9
6–7	8.14	25.1	44.7	60.5	71.3	78.4	82.8	85.6	87.2	88.1	88.8	89.1
5–6	8.12	25.0	44.3	59.9	70.3	77.0	81.2	83.7	85.1	86.0	86.6	86.9
4–5	8.09	24.8	43.9	58.9	68.8	75.1	78.9	81.2	82.4	83.1	83.7	83.9
3–4	8.05	24.6	43.1	57.4	66.5	72.2	75.5	77.4	78.5	79.1	79.5	79.7
2–3	8.00	24.1	41.7	54.6	62.5	67.2	69.9	71.4	72.2	72.6	72.9	73.0
1–2	7.86	23.0	38.5	48.9	54.9	58.2	60.0	60.9	61.4	61.7	61.9	61.9
0–1	7.42	19.6	29.8	35.3	38.2	39.7	40.4	40.8	40.9	41.0	41.1	41.1

The original motivation for plotting the data in the manner of Fig. 2 was the suggestion made by Jenkins *et al.*[14] that the fraction of the energy escaping an infinitely long cylinder, when plotted versus the radius in Molière units, might form a universal curve. The data measured previously in copper, tin, and lead targets with a CsI(Tl) detector yielded curves which fell farther away from the Nagel prediction the lower the atomic number of the target material. The behavior of the water data measured with two different detectors indicates that the apparent dependence on atomic number of the target is at least in part a detector-dependent result.

Of all the materials investigated using the CsI(Tl) detector, tin with an atomic number of 50 is the best match and would be expected to yield the most realistic results. If the concept of the "universal" radial escape curve were to be meaningful, then it would be expected that the data measured in tin with the CsI(Tl) detector and in water with the anthracene detector should coincide with each other and with the radial escape curve calculated for lead by Nagel.

The curves are not the same, and the differences are outside the experimental and calculational uncertainties. Moreover, the radial escape curve measured in aluminum with a CaF_2(Eu) detector is found to coincide with the tin curve, even though the match between CaF_2(Eu) and aluminum is as poor as the match between CsI(Tl) and copper. And the previously measured radial escape curve for copper was found to lie significantly above the tin curve.

Conclusions

The results of the present and previous experiments lead to several conclusions. The data verify that the mechanism by which energy is deposited at the initiation of the shower is ionization of the target media. The data also indicate that the shower component by which energy is propagated at depths beyond shower maximum is γ rays, the energy of which lies between the minima in the attenuation and in the absorption curves.

While the measured longitudinal distribution of energy deposition is relatively insensitive to the atomic number of the detector (for the small detectors employed in this experiment), the measured lateral distribution of energy deposition is strongly dependent on the detector used. No simple picture explains all the data, but the data indicate that the radial distribution of energy deposition is wider, for all materials studied so far (see Ref. 7) than that predicted by Nagel. The only exceptions to this are the data measured by Jenkins *et al.*[14] in lead and copper. However, they employed a LiF detector which is of much too low an atomic number for these target media.

A question posed by this experiment is what mechanisms, neglected in Nagel's calculations, are responsible for the differences between the theoretical curve and these data. One component of electromagnetic cascades neglected in the calculations is annihilation γ rays. The inclusion of this energy transport mechanism in the Monte Carlo calculations may produce results which are more consistent with the measured data.

ACKNOWLEDGMENTS

The authors wish to thank Professor Robert Hofstadter and Professor Mason Yearian for making available the accelerator and facilities of the High Energy Physics Laboratory, Stanford University. We also wish to thank Werner Wadensweiler and Len Birkwood for implementing the development of the automatic data-acquisition system; Marinus Ryneveld for preparing programs for the on-line data-acquisition system; Robert Parks for designing the target and detector assemblies; Sal Bravo, Alvin Cullins, and John Reese for constructing the apparatus; and all the staff of the High Energy Physics Laboratory for assisting us to perform this experiment and to prepare this manuscript. Finally, we would like to thank Dr. Howard Reiss of the Naval Ordnance Laboratory for assisting with the reduction of the data and C. R. Gillespie of Louisiana State University for assisting with the data acquisition.